

# The Effect of Solute Elements on Hardness and Grain Size in Platinum Based Binary Alloys

Taichi Murakami\*<sup>1</sup>, Ryoji Sahara\*<sup>2</sup>, Daisuke Harako\*<sup>3</sup>, Masahiro Akiba\*<sup>4</sup>,  
Takayuki Narushima and Chiaki Ouchi

Department of Materials Processing, Tohoku University, Sendai 980-8579, Japan

The effects of 25 kinds of solute elements on hardness and grain size in annealed Pt-based binary alloys were investigated together with cold workability and a hardness variation with a cold rolling reduction. Grain size largely varied depending on solute elements and their concentrations, and so the decrement in grain size per 1 at% solute addition was evaluated based on grain size difference between pure platinum and a respective alloy. This value markedly reduced in the low solute concentration range below 5 at%, followed by a sluggish reduction in the higher solute concentration range. Hardness values obtained in all alloys were corrected considering contribution of hardening due to grain refinement, and solid solution hardening was evaluated by the increment in hardness per 1 at% solute addition. The lattice constants of pure platinum and alloys were measured to calculate the size misfits. The increment in hardness increased with the increase in the size misfit in all alloys, and this relationship was clearly divided into two groups depending on whether the binary alloy system is a completely miscible type or a type with the solubility limit. The increment in hardness in the latter type of alloys was much higher than that of the former, and this value became larger with the increase in the inverse value of the solubility limit in Pt-based binary alloy. The superior cold workability and very similar work hardening behavior were observed in all Pt-based binary alloys. [doi:10.2320/matertrans.MRA2007265]

(Received October 31, 2007; Accepted December 5, 2007; Published January 23, 2008)

**Keywords:** platinum based binary alloy, solid solution hardening, grain size, misfit parameter, cold workability, work hardening

## 1. Introduction

Pure platinum and its alloys are currently used in a wide variety of application fields because of their several superior properties over other metals and alloys. Pure platinum is a very soft and ductile metal with Vickers hardness of around 50 in  $H_V$ , and possesses excellent cold workability.<sup>1,2)</sup> Platinum and its alloy are also used as a catalyst for purification of exhaust gas and crude oil. This metal has superior corrosion resistant property in various corrosive environments at both ambient and high temperatures, resulting in a wide use as a refractory material such as a crucible or a mold, and as a component material used in various laboratory equipments.<sup>2,3)</sup>

One of the largest markets of platinum is jewelry and ornaments. Platinum jewels such as rings, bracelets and necklaces are manufactured by both routes of precision casting and wrought processes.<sup>2,4)</sup> In general, jewelry products made by noble metals and alloys are manufactured through various processes such as forming, machining, cutting or polishing.<sup>4)</sup> In particular, extremely fine cutting and polishing are the most important to achieve attractive surface appearance in these applications. Similarly to other noble pure metals, pure platinum is too soft to accomplish very fine surface appearance by polishing, and it also tends to suffer a surface damage such as scratch or dent during use, deteriorating excellent surface appearance. Thus, hardening or strengthening by addition of alloying elements into noble metals is

primarily conducted to solve this problem, and in fact, the most practical noble alloys for jewelry application contain various alloying elements in the total contents ranging from 5 to 25 mass%.

The selection and the amount of addition of alloying elements in noble metals for jewelry application have been conducted by considering several factors besides hardening such as modification of surface color appearance, cost of alloying additives, biocompatibility, manufacturing conditions or easiness in recycle of the base metal. New noble alloy development for jewelry application has been conducted mostly by an experience-based method, which is particularly true in platinum-based alloys. Platinum has a relatively short history of industrial use since a large-scale exploitation of platinum started in 1920's, and this metal is the most expensive among noble metals. As a result, very few systematic studies have been performed regarding on the effect of alloying elements on various properties in platinum-base alloys in the past. Currently, Biggs *et al.* reported hardening of platinum alloys for jewelry application,<sup>4)</sup> and Pt-based intermetallic alloys have been studied with aiming the development of the more superior high temperature material over Ni-based super-alloys.<sup>5-8)</sup>

Under these circumstances in platinum alloys, the present study was conducted to investigate systematically the effect of various solute elements on hardness and grain size in platinum-base binary alloys. Grain refinement by addition of solute elements is important in both of cast and wrought products, because the microstructure with coarse grains deteriorates not only mechanical property, but also surface appearance of cold worked products with a fine surface finish. Total numbers of 25 kinds of solute elements belonging to the group number from 3 to 14 and the periodic number from 3rd to 6th in the periodic table were investigated, and a respective solute element was added in the concentration range of solid solution in platinum-base binary alloy with FCC structure.

\*<sup>1</sup>Present address: Institute of Multidisciplinary Research for Advanced Materials, Tohoku University, Sendai 980-8577, Japan

\*<sup>2</sup>Present address: Institute for Materials Research, Tohoku University, Sendai 980-8577, Japan

\*<sup>3</sup>Undergraduate Student, Tohoku University, Present address: JFE steel, Steel Research Center, Chiba 260-0835, Japan

\*<sup>4</sup>Undergraduate Student, Tohoku University, Present address: TOPCON CORPORATION, Tokyo 174-8580, Japan

Table 1 Solute elements and their concentrations in Pt-based binary alloys used in this study, which are listed on the periodic table. The upper row: the solute element, the bottom row: the concentration in mass%

Period number	Group number											
	3	4	5	6	7	8	9	10	11	13	14	
3											Al	
											0.5	
4	Sc	Ti	V	Cr	Mn	Fe	Co	Ni	Cu			Ge
	0.5	1.49	2.5, 4.0	6.0	2.5	2.5	2.5	2.5	2.0, 4.5, 8.0	5.0		0.5
5		Zr	Nb	Mo		Ru	Rh	Pd			In	Sn
		2.5, 5.0	2.5	2.5		10.8	5.0	20.0			2.5	2.5
6		Hf	Ta	W	Re		Ir			Au		
		0.5	2.5	2.5	2.5		5.0, 10.0, 15.0			5.0		

Grain size and hardness measurements in annealed alloys were primarily conducted, and work hardening behavior in pure platinum and Pt-based binary alloys was also conducted by investigation of hardness variations with a rolling reduction in cold rolling. The solute concentrations among various binary alloys prepared in this study were largely different, and thus evaluations of grain refinement and solid solution hardening due to a respective solute element were conducted based on calculations of the decrement in grain size and the increment in hardness per 1 at% solute addition, respectively. The increment in hardness in various Pt-based binary alloys was analyzed and discussed based on the misfit parameter which was calculated from the lattice constants measured by X-ray diffraction (XRD).

## 2. Experimental Procedure

Platinum based binary solid solution alloys were prepared using argon arc melting furnace with a water-cooled copper mold and a non-consumable electrode. Total numbers of 25 kinds of elements were selected as additives of Pt-based solid solution alloys, excluding toxic or radio-active elements and high vapor pressure elements. As shown in Table 1, solute elements and their concentrations in Pt-based alloys are listed on the periodic table. The concentration in a respective solid solution alloy prepared in this study was mostly one level, and it was near to the solubility limit of Pt-based binary alloy except alloys containing V, Ni, Zr and Ir. Solute concentrations in these alloys were varied in two or three levels to examine grain size and hardness variations with concentrations. The concentration in Pt-X alloy noted hereafter is mass% except the case noted otherwise.

Melting raw materials used were pure platinum sheet with 1 mm in thickness and purity of 99.9%. Additives had various shapes such as powder, flake, sheet or grain, and their purity was 99.9% except vanadium, iron and zirconium of which purity was 99%. Special cautions were taken in both preparations of melting raw materials and melting procedures. The mass of pure platinum or additives was precisely measured, and additives were enclosed by platinum foil. The melting was repeated for 4 times, and contamination during melting was minimized. The mass loss during melting was very tiny, being less than 1% in all ingots. Chemical compositions of ingots were not analyzed, but nominal compositions calculated based on both masses of platinum

and an additive element used in preparation of a respective ingot were used for data presentations and analysis. The mass of a button ingot was around 9 g, and the ingot size was 10 mm in diameter and 6 mm in thickness.

Button ingots were homogenized at 1573 K for 18 ks under argon gas atmosphere, and subsequently isothermal hot-compression was conducted under vacuum using a hot working simulator of THERMECMAS-MASTER-Z. Ingots were deformed from 6 mm to 3 mm in the thickness direction at the temperature of 1573 K and strain rate of  $2 \times 10^{-3} \text{ s}^{-1}$ . Hot-deformed alloys were subsequently hot-rolled to 1.5 mm thickness after reheating at 1373 K. Finally, alloys were annealed at 1373 K for 3.6 ks under argon gas atmosphere. Annealed specimens with the initial thickness of 1.5 mm were cold-rolled with various rolling reductions of approximately 20, 50 and 70%. Hardness of both of annealed and cold rolled specimens was measured using a Vickers hardness tester (Akashi corp. MVK-H1) with a load of 1 kgf.

Microstructural observations and hardness measurements were performed in the center part of the cross section in the specimens which were halved by cutting in the thickness direction. The microstructure of the annealed specimen was revealed by etching in use of a nitro-hydrochloric acid solution at 323 K and was observed by an optical microscopy. Grain size was measured by an intercept method. The lattice constant value was measured by X-ray diffraction (RIGAKU Corp., RINT-2200). Diffraction peaks were determined using  $\text{CuK}\alpha_1$  and  $\text{CuK}\alpha_2$  radiations, and seven diffraction peaks were measured and used for analysis. Tiny errors are involved in measurements of diffraction peaks or  $2\theta$ , and thus, the true lattice constant of  $a_0$  was obtained by calibrating measured lattice constant values using eq. (1),<sup>9)</sup>

$$a = a_0 + a_0 K \cos^2 \theta \quad (1)$$

where  $a$  and  $2\theta$  are the measured lattice constant and Bragg angle obtained from a respective diffraction peak, respectively. The value of  $a_0$  was obtained by extrapolating  $\cos^2 \theta$  to zero in plots of  $a$  vs  $\cos^2 \theta$ . Accuracy of the lattice constant value was within  $\pm 0.0001$  nm.

## 3. Results

### 3.1 The effect of solute elements on grain size of Pt-based binary alloys

The microstructures evolved in annealed pure platinum

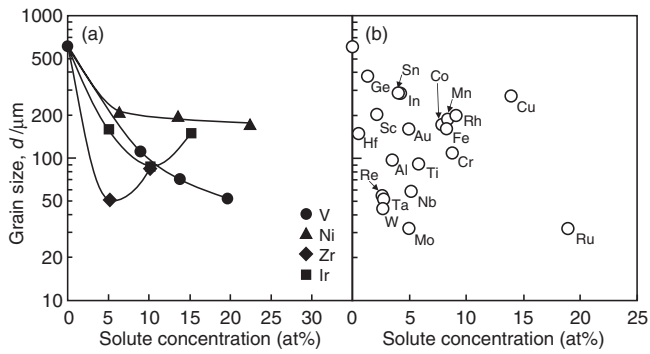


Fig. 1 Variations of grain size with the solute concentration in Pt-based alloys in (a), and grain size in a solute concentration in a respective Pt-based alloy in (b).

and Pt-based binary alloys exhibited all equiaxed structure. Values of grain size obtained in annealed pure platinum and all binary alloys are summarized in Table 1. In Fig. 1, values of grain size obtained in pure platinum and all binary alloys are plotted against the solute concentration in atomic % in a respective alloy, where the vertical axis of grain size is expressed by a log-scale. Grain size varies in a very wide range from 610  $\mu\text{m}$  in pure platinum to 33  $\mu\text{m}$  in Pt-2.5% Mo or Pt-10.8% Ru alloy. Figure 1(a) shows variations of grain size with concentrations of V, Ni, Zr and Ir. The marked grain refinement in the low solute concentration range is found in all of these alloys. In the higher solute concentration range, grain refinement tends to sluggish in Ni- and V-added alloys, and grain size in Ir- and Zr-added alloys increases with the increase of the solute concentration after yielding the minimum value of grain size. Figure 1(b) shows grain size in a respective solute concentration in other binary alloys. Grain size in alloys with the higher solute concentration tends to become finer compared with that in alloys with the lower solute concentration, but grain size at a given solute

concentration shows a wide variation depending on solute elements.

Several examples of the microstructures evolved in pure platinum and various Pt-based binary alloys are shown in Fig. 2. Grain size changes from 610  $\mu\text{m}$  in pure platinum to 51  $\mu\text{m}$  in Pt-2.5%Zr alloy. The solute concentration is largely different among various binary alloys, and so the decrement in grain size per 1 at% solute addition was calculated in all binary alloys based on the equation of  $(D_{\text{Pt}} - D_{\text{Pt-X}})/(\text{atomic solute concentration in Pt-X alloy})$ , where  $D_{\text{Pt}}$  and  $D_{\text{Pt-X}}$  are grain size of pure platinum and Pt-X alloy, respectively. Grain size and calculated values of the decrement in grain size in all alloys are listed in Table 2.

Decrements in grain size per 1 at% solute addition in all binary alloys are graphed in Figs. 3(a) to (d), where the solute element in a respective alloy is put side by side based on periodic numbers of 3rd, 4th, 5th and 6th, respectively. Solute elements in each periodic number are put in order of the group number from the left to right sides, and difference in crystal structures of a respective element is also expressed by different marks. The decrement in grain size in V-, Ni-, Zr- or Ir-added alloy shown in this graph is the value obtained in the least solute concentration in a respective alloy. Solute elements belonging to the 6th period number evidently give rise to the largest decrement in grain size, and the smallest decrement is observed in solute elements belonging to 4th period. It is also found that solute elements belonging to the lower group number in a respective periodic number yield the larger decrement in grain size compared with solute elements with the higher group number. Elements belonging to lower group numbers such as Hf, Ta, W, Re, Zr, Nb or Ti have mostly BCC or HCP structure, and these solute elements result in the larger decrement in grain size compared with elements with FCC structure such as Ni, Cu or Au. The largest decrement in grain size is obtained by Hf addition of 0.5 at%, which was 838  $\mu\text{m}$  per 1 at% addition and the second ranked elements in a strong grain refiner are W, Re and Ta, of

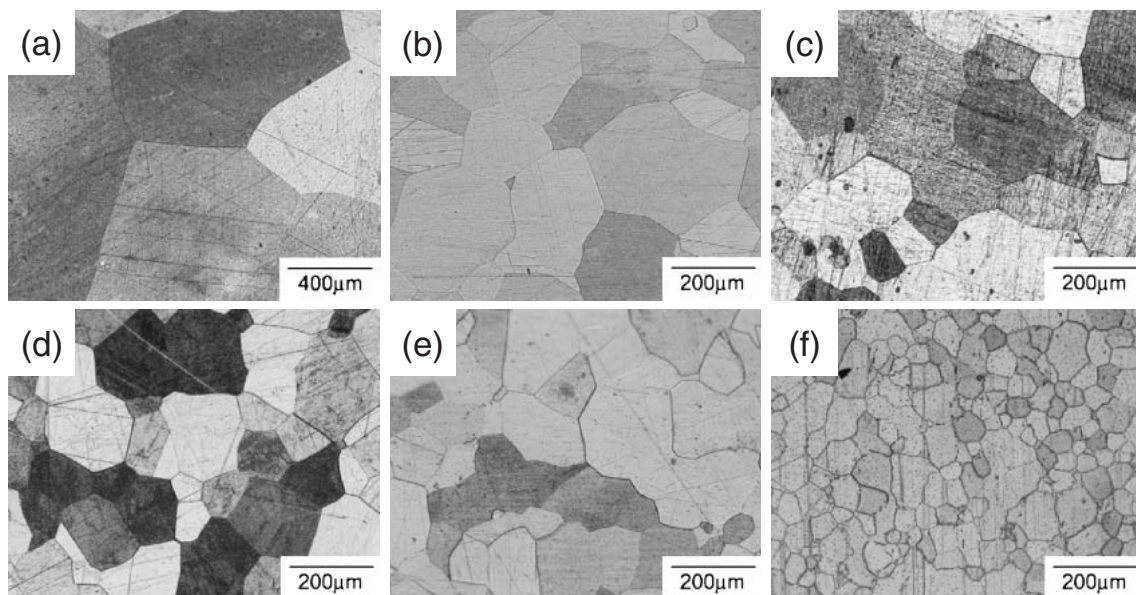


Fig. 2 Optical micrographs of pure platinum in (a) and Pt-X binary alloys from (b) to (f). Solute elements, X are (b) 2.5% In, (c) 4.4% Ni, (d) 5.0% Rh, (e) 2.5% V and (f) 2.5% Zr.

Table 2 Grain size and hardness obtained in Pt-based binary alloys.

No	Element	Periodic table		Concentration		Grain size (D)		Hardness (H <sub>v</sub> )		
		Period	Group	(mass%)	(atomic %)	( $\mu\text{m}$ )	( $\Delta D$ )/at%	Measured	Calibrated	( $\Delta H_v$ )/at%
1	Al	3	13	0.5	3.5	100	145	72	60	2.8
2	Sc	4	3	0.5	2.1	209	188	126	120	32.9
3	Ti	4	4	1.49	5.8	94	89	162	149	17.1
4	V	4	5	2.5, 4.0, 6.0	8.9, 13.8, 19.6	111, 71, 52	56, 39, 28	164, 186, 219	153, 170, 199	11.5, 8.7, 7.6
5	Cr	4	6	2.5	8.8	112	57	124	113	7.2
6	Mn	4	7	2.5	8.3	193	50	121	115	7.7
7	Fe	4	8	2.5	8.2	167	54	121	113	7.7
8	Co	4	9	2.5	7.8	178	55	105	98	6.1
9	Ni	4	10	2.0, 4.5, 8.0	6.4, 13.5, 22.4	205, 192, 168	64, 31, 20	109, 151, 216	103, 145, 209	8.3, 7.0, 7.1
10	Cu	4	11	5	13.9	281	24	131	127	5.5
11	Ge	4	14	0.5	1.3	387	167	125	123	54.7
12	Zr	5	4	2.5, 5.0	5.2, 10.1	51, 85	108, 52	212, 405	192, 370	27.3, 31.7
13	Nb	5	5	2.5	5.1	60	108	136	118	13.3
14	Mo	5	6	2.5	5.0	33	116	135	108	11.7
15	Ru	5	8	10.8	18.9	33	31	198	171	6.4
16	Rh	5	9	5	9.1	205	45	78	72	2.4
17	Pd	5	10	20	32.2	284	10	79	75	0.8
18	In	5	13	2.5	4.2	294	76	146	142	22.1
19	Sn	5	14	2.5	4.0	294	78	147	143	23.1
20	Hf	6	4	0.5	0.5	152	838	79	71	37.9
21	Ta	6	5	2.5	2.7	53	207	124	104	20.2
22	W	6	6	2.5	2.6	46	213	109	87	14.0
23	Re	6	7	2.5	2.6	56	212	106	87	14.1
24	Ir	6	9	5.0, 10.0, 15.0	5.1, 10.1, 15.2	160, 87	89, 52	81, 125, 165	73, 111, 157	4.6, 6.1, 7.0
25	Pt	6	10	base		610		50	50	—
26	Au	6	11	5	5.0	164	90	117	109	12

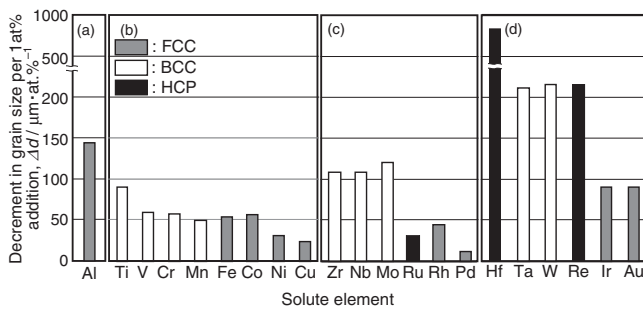


Fig. 3 Decrement in grain size per 1 at% solute addition in various solute elements shown on the periodic table.

which the decrements in grain size per 1 at% addition are 213, 212 and 207  $\mu\text{m}$  per 1 at% solute addition, respectively.

Figure 3 shows a very large variation in the decrement in grain size depending on solute elements. However, the large difference in solute concentration among various binary alloys possibly affects the decrement in grain size per 1 at% solute addition. Therefore, the relationship between decrements in grain size per 1 at% solute concentration and the solute concentration in a respective alloy is graphed as shown in Fig. 4, where the vertical axis is a log-scale. Data of all binary alloys including alloys with two or three levels of the solute concentration are included in this figure. Variations in the decrement in grain size with the solute concentration in all binary alloys are approximated by two straight bands with

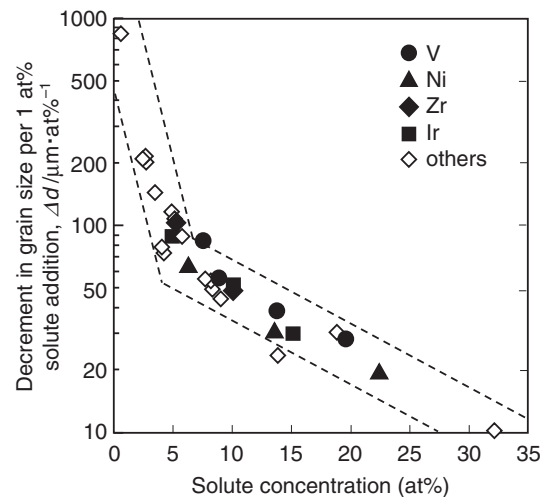


Fig. 4 Relationship between the solute concentration and the decrement in grain size per 1 at% solute addition in Pt-based binary alloys.

a bending point in a solute concentration of around 5 at%. The decrement in grain size by addition of various solutes is affected by both the solute concentration and solute elements, and the latter effect is shown by the width of straight bands. The result shown in Fig. 4 indicates that the former effect on the degree of grain refinement is much larger than the latter effect. The decrement in grain size is very large in the low solute concentration range up to approximately 5 at%, and

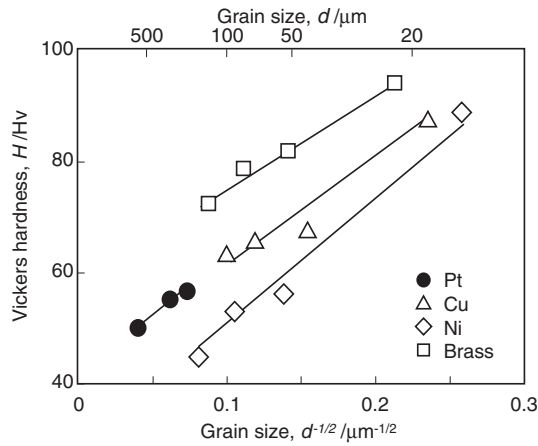


Fig. 5 Hardness variations with grain size plotted by Hall-Petch relationship in pure platinum and other FCC metals and alloy.<sup>10)</sup>

the further increase of solute concentration up to 33 at% yields a much smaller slope in a straight band in the relationship between the decrement in grain size and the solute concentration.

### 3.2 The effect of solute elements on hardness of Pt-based binary alloys

Hardness values obtained in all annealed binary alloys are listed in Table 2, which are largely varied in the range from 50 in  $H_V$  in pure platinum up to 405 in  $H_V$  in Pt-5%Zr alloy. Strength or hardness in solid solution alloys with a single phase is primarily controlled by both grain size and solid solution hardening. Because a wide variation in grain size was observed in the present Pt-based binary alloys, the value of hardness obtained in a respective alloy is needed to calibrate the amount of hardening raised by the difference of grain size for comparison of solid solution hardening among various solute elements. Therefore, grain size dependence of hardness in pure platinum was investigated. Grain size of pure platinum was varied from 182  $\mu\text{m}$  to 610  $\mu\text{m}$  by changing annealing temperatures from 973 to 1373 K, and hardness of these specimens was measured. Grain size dependence of hardness in pure platinum is shown in Fig. 5 together with that of other FCC metals and alloy reported by Wang.<sup>10)</sup> This relation is expressed by eq. (2) similarly to Hall-Petch relationship for yield strength,

$$H_{V_{\text{Pt}}} = H_{V_0} + K D_{\text{Pt}}^{-\frac{1}{2}} \quad (2)$$

where  $H_{V_0}$  is the constant value, and  $H_{V_{\text{Pt}}}$  and  $D_{\text{Pt}}$  are hardness and grain size of pure platinum, respectively. It is found from this figure that  $K$  value of pure platinum is almost the same as that of other FCC metals and alloy, and that  $H_{V_0}$  and  $K$  values are 42 in  $H_V$  and 204  $H_V \cdot \mu\text{m}^{-1/2}$ , respectively. Grain size dependence of hardness in all binary alloys was assumed to be the same as that of pure platinum, and hardness values in all alloys were calibrated using this  $K$  value under the condition that grain size in all alloys is the same as that of pure platinum. Calibrated hardness values in all binary alloys are also listed in Table 2. In the following, calibrated hardness values in alloys are used for data presentation and analysis.

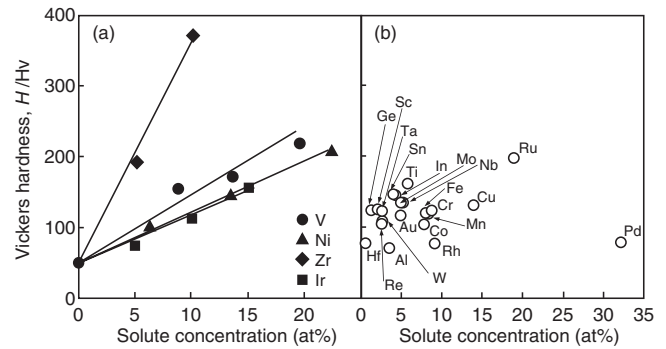


Fig. 6 Variations of hardness with the solute concentration in Pt-based binary alloys in (a) and hardness in a solute concentration in a respective binary alloy in (b).

Figure 6(a) shows variations of hardness in V-, Ni-, Zr- and Ir-added binary alloys with the solute concentration in at%. The best data fitting was obtained by the linear plot of the solute concentration in the horizontal axis except V, although data plots based on the 1/2 or 2/3 power of the concentration were examined. Hardness in a respective alloy changes linearly with the solute concentration, and addition of Zr results in much larger hardening over other three solute elements. Figure 6(b) shows the effect of other solute elements on hardness in a respective amount of addition in binary alloys. It is found that and calibrated hardness values are dispersed in the range from 50 to 171 without depending on the solute concentration in a respective binary alloy.

Similarly to grain size variations due to addition of various solutes, the increment in hardness per 1 at% solute addition was calculated based on the equation of  $(H_{V_{\text{Pt-X}}} - H_{V_{\text{Pt}}}) / (\text{atomic solute concentration in Pt-X alloy})$ , where  $H_{V_{\text{Pt-X}}}$  and  $H_{V_{\text{Pt}}}$  are hardness values of Pt-X alloy and pure platinum, respectively. Calculated values of the increment in hardness per 1 at% solute addition are listed in Table 2. Figures 7(a) to (d) show increments in hardness per 1 at% solute addition in all binary alloys, where the solute element in a respective alloy is put side by side based on the periodic table similarly to Fig. 3. All solute elements give rise to hardening, although such elements as Pd and Rh yield a very tiny hardening. Top three-ranked solute elements in the largest increment in hardness per 1 at% solute addition are Hf, Zr and Sc, which belong to the lowest group number in periodic numbers of 5th, 4th and 3rd, respectively. The increment in hardness per 1 at% solute addition tends to become larger with a reduction of group number in a respective periodic number, but the periodic number appears to have no relationship with the increment of hardness. Solute elements with FCC structure yield the least hardening among solutes with various crystal structures. The datum of Ge is excluded in this figure, but this element belonging to the group number of 14th result in the largest increment in hardness among all alloys as seen in Table 2. This result indicates that the ranking of the increment in hardness among various solutes in binary alloys can not be fully explained based on the periodic group number. This result of Ge is used in the analysis conducted in the following chapter.

Similarly to Fig. 4 showing dependence of the decrement in grain size on the solute concentration, the relationship



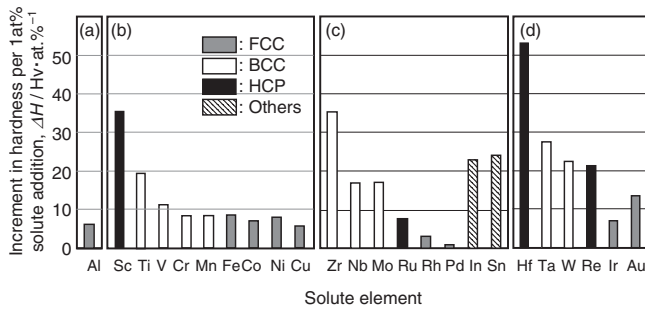


Fig. 7 Increment in hardness per 1 at% solute addition in various solute elements shown on the periodic table. Solute elements shown from (a) to (d) belong to the 3rd, 4th, 5th and 6th periodic numbers, respectively.

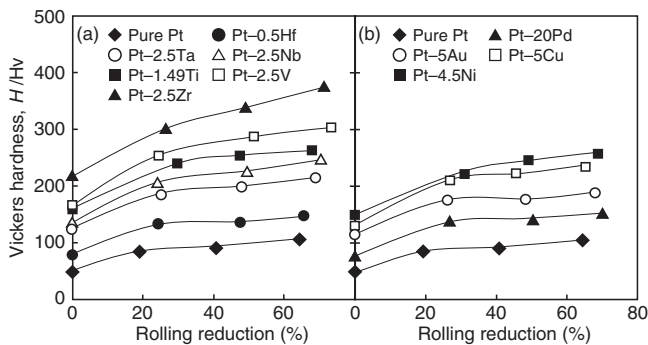


Fig. 8 Variations of hardness with a cold rolling reduction in pure platinum and Pt-based binary alloys. Solute elements shown in (a) and (b) belong to group numbers of 4th and 5th, and 10th and 11th, respectively in the periodic table.

between the increment in hardness per 1 at% solute addition and the solute concentration in a respective alloy was examined. However, data scatter in this relationship was very large and any distinct relationship was not observed. Solid solution hardening or the increment in hardness is analyzed based on the size misfit in the following chapter.

### 3.3 Hardness variations with a cold rolling reduction

Hardness variations with a cold rolling reduction in pure platinum and binary alloys were investigated by changing the rolling reduction up to 70%. All alloys showed an excellent cold workability without suffering any cracking even in the high rolling reduction. Figures 8(a) and (b) show results of pure platinum and binary alloys with elements belonging to group numbers of 4th and 5th, and 10th and 11th in periodic table, respectively. A relatively high work hardening rate is observed in a rolling reduction up to 20 or 25% in pure platinum and all binary alloys, and the work hardening rate tends to become low with a further extension of a rolling reduction. Hardness of pure platinum which is 50 in  $H_V$  in as annealed condition becomes over 100 in  $H_V$  in a rolling reduction of approximately 60%. No marked difference in work hardening rate appears to be observed among elements classified by a respective group number. All binary alloys exhibit very similar work hardening behavior to that of pure platinum, although a quantitative analysis of work hardening rate in a respective binary alloy was not conducted. The work hardening due to cold rolling in pure platinum and binary

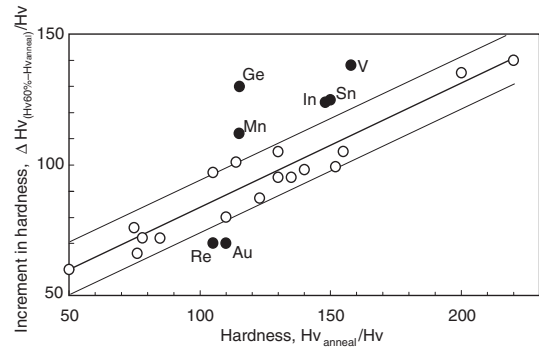


Fig. 9 Relationship between hardness in annealed condition and the increment in hardness after cold rolling with a reduction of 60% in Pt-based binary alloys.

alloys was evaluated based on the difference in both hardness values obtained after cold rolling with a rolling reduction of 60% and after annealing. Figure 9 shows the relationship between hardness in as annealed condition and the increment in hardness after cold rolling with 60% rolling reductions. The increment in hardness in the most alloys increases linearly with the increase of hardness obtained by annealing except several alloys, of which the relationship is expressed by eq. (3).

$$\Delta H_V = 36.5 + 0.47H_{V_{\text{anneal}}} \quad (3)$$

where  $\Delta H_V$  is the difference of hardness values after cold rolling with a rolling reduction of 60% and annealing, and  $H_{V_{\text{anneal}}}$  is hardness in as annealed condition. Cold working under a strict control of the rolling reduction is one of methods for strengthening or hardening metals and alloys, and therefore it is expected that such data as shown in Figs. 8 and 9 can be utilized for strengthening or hardening of pure platinum and platinum-based binary alloys.

## 4. Discussion

### 4.1 The effect of solute elements on grain size in Pt-based binary alloys

In this study, the solute concentration in a respective binary alloy was largely different, and so the effect of various solute elements on grain size was evaluated based on the decrement in grain size per 1 at% solute addition. This value showed a strong dependence of the solute concentration in a respective alloy, while the effect of the solute element on this value was relatively small. The least solute addition resulted in the largest decrement in grain size, and the increase in the solute concentration up to around 5 at% decreased this value at the high rate, followed by a sluggish reduction of this value with the further increase in the solute concentration over 5 at%. The effect of the substitutional solute element on grain growth has been explained based on solute drag mechanism, where grain boundary mobility is controlled by the solute element segregated on grain boundary or dispersed nearby grain boundary.<sup>11)</sup> As solubility of the solute element in the grain boundary is very limited, grain boundary mobility reduces more markedly in the leaner solute concentration. This induces the larger decrement in grain size in the leaner solute concentration. Togashi *et al.* reported the effect of the

content of various substitutional alloying elements on the mobility of the  $\alpha/\gamma$  interface in C-Mn steel, where the interface mobility reduced at very high rate in the range of very low alloy contents, followed by a sluggish reduction with the further increase of contents.<sup>12)</sup> This behavior in the relationship between the interface mobility and the content of alloying elements is very similar to the present result of a variation of the decrement in grain size with the solute concentration obtained in Pt-based binary alloys.

As shown in Fig. 3, the effect of various solute elements on the decrement in grain size per 1 at% solute addition appeared to be associated with the periodic and group numbers on the periodic table to which the solute element belonged as well as crystal structure of the solute elements. However as already noted, the analysis based on dependence of the decrement in grain size per 1 at% solute addition on the solute concentration yielded a relatively small effect of solute elements. The d-electron character of the solute element can be read from the periodic table, which affects various physical and chemical natures of the solute element. This may yield somewhat the indirect relationship between the grain refinement and the periodic and group numbers of the solute element. However, the more detail investigations are needed to reconfirm these findings and to pursuit the cause for these correlations.

#### 4.2 Solid solution hardening due to various solute elements in Pt-based binary alloys

All solute elements investigated in this study showed solid solution hardening, and any solute element causing alloy softening was not found in Pt-based binary alloys. This is in contrast to the result of austenitic stainless steel with the same FCC structure, because strength of this alloy was decreased by addition of alloying elements such as Mn, Ni or Cu, while Si and Mo additions increased strength.<sup>13)</sup> Solid solution hardening due to the substitutional element is caused by the elastic interaction between an edge dislocation and solute atoms. This elastic interaction has the size and the modulus effects, which are caused by the difference of the atomic radius and the elastic modulus, respectively. As the influence of the former is far-reaching, solid solution hardening is mostly analyzed based on the size effect.<sup>14)</sup> The size misfit parameter of a solute element,  $\varepsilon_a$  which is the ratio of a lattice constant variation per 1 at% solute addition, can be expressed by eq. (4).

$$\varepsilon_a = \frac{1}{a_{\text{Pt}}} \left| \frac{da}{dc} \right| \times 100 \quad (4)$$

where  $a$  and  $a_{\text{Pt}}$  are the lattice constants of Pt-X solid solution alloy and pure platinum, respectively, and  $|da/dc|$  is an absolute value of the slope in the straight relationship between lattice constant of  $a$  and the solute concentration of  $c$ . The other way to evaluate the size misfit is based on the difference of the atomic radius between the base metal and the solute element, which is expressed by eq. (5).

$$\varepsilon_r = \left| \frac{(r_x - r_{\text{Pt}})}{r_{\text{Pt}}} \right| \times 100 \quad (5)$$

where  $r_{\text{Pt}}$  and  $r_x$  are atomic radius of platinum and the solute element of X, respectively. The lattice constants in Pt-based

binary alloys were measured by XRD analysis, and these values are summarized in Table 3 together with calculated values of  $\varepsilon_a$ . Values of atomic radius in a respective element and calculated values of  $\varepsilon_r$  are also listed in this table together with the type of the phase diagram and the maximum solubility limit in binary alloy system. The lattice constant of pure platinum was  $0.39250 \pm 0.00005$  nm, which agreed well with the reported one.<sup>15)</sup> Figures 10(a) and (b) show variations in the lattice constant with a solute concentration in binary alloys with two levels and a single level of the solute concentration, respectively. The former figure includes the result of Pt-5%Nb alloy which was additionally prepared only for evaluation of the lattice constant. It is found from Fig. 10(a) that the lattice constants linearly change with the increase of the concentration in all solute elements. Nb and Zr increase the lattice constant, and V, Ni and Ir decrease this value. Figure 10(b) shows the lattice constants in binary alloys with a single level of the solute concentration. All solute elements besides Hf, Ta and Au decrease the lattice constant, and Co among them results in the largest reduction of the lattice constant.

Calculated values of  $\varepsilon_a$  and  $\varepsilon_r$  are shown in Table 3, where values of  $\varepsilon_a$  and  $\varepsilon_r$  are not shown by the absolute value but by the positive or negative value corresponding to actual variations of the lattice constant and the atomic radius. It is found that all solute elements having a larger atomic radius than that of platinum or a positive value of  $\varepsilon_r$  result in positive values of  $\varepsilon_a$ , and solute elements having a smaller atomic radius than that of platinum or negative values of  $\varepsilon_r$  show negative values of  $\varepsilon_a$ . Figure 11 shows the correlation between both absolute values of the size misfits of  $\varepsilon_a$  and  $\varepsilon_r$ . An excellent correlation between both values is observed except solute elements of Mn and Zr. Therefore, the increment in hardness per 1 at% solute addition in Pt-based binary alloys is analyzed using the size misfit of  $\varepsilon_a$  in the following.

Solid solution hardening in many alloy systems had been studied during the past half century, of which results were mostly analyzed based on the size misfit. King reported quantitative size-factors defined in terms of the effective atomic volume of the solute for 469 substitutional solid solutions using lattice parameter data available in the literatures, and discussed the application of these size-factors in relation to various properties of solid solution alloys.<sup>16)</sup> He introduced the linear size-factor and calculated this value of many solid solution alloys. For various solute elements in Pt-based binary alloys, the correlation between the linear-size factors calculated by King and the size misfit obtained in the present study is shown in Fig. 12, where an excellent correlation between them is found.

Figure 13 shows the relationship between the increment in hardness per 1 at% solute addition and the size misfit of  $\varepsilon_a$  in Pt-based binary alloys, where the vertical scale is a log-scale. Lattice constants of Sc, Ti, Ge and Mo were not measured. So, increments in hardness in these solutes were plotted using  $\varepsilon_r$  values in place of  $\varepsilon_a$  in this figure, where these solutes were shown in the different mark. The correlation between them is clearly classified into two groups depending on a type of phase diagram in Pt-X binary alloy system. In the most of a completely miscible type of alloys except Pt-Au and Pt-Ir

Table 3 Classification of alloy type, the maximum solubility limit, the measured lattice constant and  $\epsilon_a$  in Pt-based alloys, and atomic radius and  $\epsilon_r$  of the solute element.

No	Element	Alloy type in Pt-X	Solubility limit (at%)	Concentration		Lattice const. (nm)	$\epsilon_a$ (%)	Atomic radius (nm)	$\epsilon_r$ (%)
				(mass%)	(atomic %)				
1	Al	Eutectic	16.2	0.5	3.5			0.1431	3.70
2	Sc	Peritectic	12.0	0.5	2.1			0.1606	16.38
3	Ti	Peritectic	17.7	1.5	5.8			0.1448	4.93
4	V	Eutectic	57.4	2.5	8.9	0.39070	-4.94	0.1321	-4.28
5	Cr	Eutectic	75.3	6.0	19.6	0.38872	-6.11	0.1249	-9.49
6	Mn	Eutectic	38.0	2.5	8.3	0.39161	-2.69	0.1240	-10.14
7	Fe	Miscible		2.5	8.2			0.1241	-10.07
8	Co	Miscible		2.5	7.8	0.39020	-7.49	0.1253	-9.20
9	Ni	Miscible		4.5	13.5	0.38870	-7.19	0.1246	-9.71
10	Cu	Miscible		8.0	22.4	0.38615			
11	Ge	Peritectic	6.7	5.0	13.9	0.38912	-6.18	0.1278	-7.39
12	Zr	Peritectic	22.6	0.5	1.3			0.1225	-11.23
13	Zr	Peritectic	22.6	2.5	5.2	0.39401	6.77	0.1600	15.94
14	Zr	Peritectic	22.6	5.0	10.1	0.39512			
15	Nb	Peritectic	20.6	2.5	5.1	0.39282	1.76	0.1429	3.55
16	Nb	Peritectic	20.6	5.0	10.0	0.39320			
17	Mo	Peritectic	44.2	2.5	5.0			0.1362	-1.30
18	Ru	Peritectic	70.0	10.8	18.9	0.39002	-3.34	0.1340	-2.90
19	Rh	Miscible		5.0	9.1	0.39137	-3.17	0.1345	-2.54
20	Pd	Miscible		20.0	32.2	0.39114	-1.08	0.1376	-0.29
21	In	Peritectic	11.3	2.5	4.2			0.1626	17.83
22	Sn	Eutectic	13.8	2.5	4.0			0.1405	1.81
23	Hf	—	11.0	0.5	0.5	0.39277	12.64	0.1564	13.33
24	Ta	Peritectic	19.0	2.5	2.7	0.39263	1.23	0.1430	3.62
25	W	Peritectic	65.0	2.5	2.6	0.39226	-2.22	0.1370	-0.72
26	Re	Peritectic	42.0	2.5	2.6	0.39226	-2.32	0.1370	-0.72
27	Ir	Miscible		5.0	5.1	0.39226	-1.50	0.1357	-1.67
28	Ir	Miscible		10.0	10.1	0.39186			
29	Au	Miscible		5.0	5.0	0.39310	3.12	0.1442	4.49

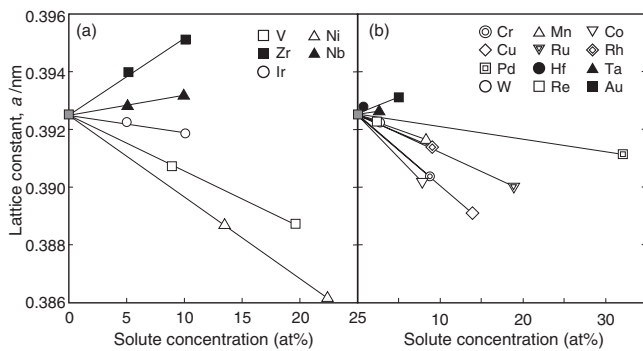


Fig. 10 Variations of the lattice constant with the solute concentration in Pt-based binary alloys. Solute elements shown in (a) and (b) belong to group numbers from 4th to 7th, and from 8th to 11th, respectively in the periodic table.

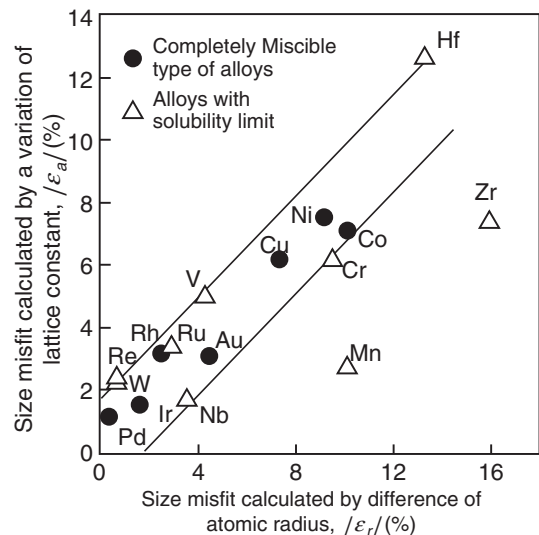


Fig. 11 Relationship between both size misfits calculated by difference of the atomic radius and a variation of the lattice constant in Pt-based binary alloys.

alloy systems, the logarithm of the increment in hardness increases linearly with the increase of the absolute value of the size misfit. Increments in hardness in Pt-Au and Pt-Ir alloys were much larger than values inferred from the relationship between the increment in hardness and the misfit for a completely miscible type of alloys. This may be caused by additional hardening due to the order phase which may be formed during cooling in annealing treatment. The increment

in hardness in alloys with the solubility limit which are shown by open marks in this figure also increases with the size misfit, although this correlation yields a wider band of



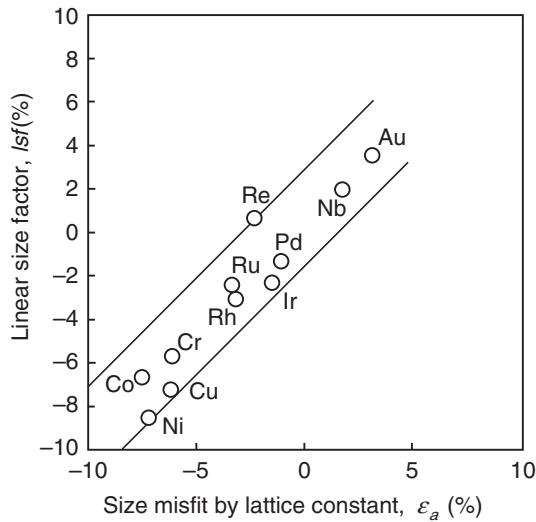


Fig. 12 Relationship between the linear size factor reported by King<sup>16)</sup> and the size misfit obtained in this study in Pt-based binary alloys.

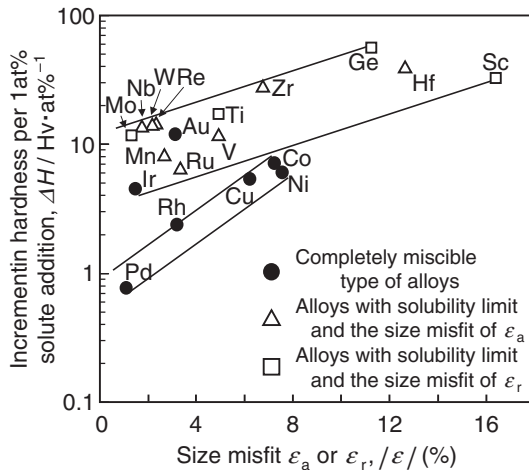


Fig. 13 Relationship between the size misfit and the increment in hardness per 1 at% solute addition in Pt-based binary alloys.

data scatter than that in a completely miscible type of alloys. The increment in hardness in this type of alloys is always larger than that of a completely miscible type of alloys. Consequently, it was found in Pt-based binary alloys that solid solution hardening in alloy systems with the solubility limit was much higher than that in a completely miscible type of alloys, while solid solution hardening in both types of alloys was primarily controlled by the size misfit.

Suzuki's group studied solid solution hardening in Ni-X binary alloys and Ni-40 at%Co-X ternary alloys, reporting that solid solution hardening in alloys with the solubility limit became larger than that of alloys with a completely miscible similarly to the present result.<sup>17-19)</sup> It was also reported that an extra hardening observed in the former type of alloys increased with a reduction of the solubility limit. Thus, in the present Pt-based binary alloys, the relationship between the increment in hardness and an inverse of the solubility limit in a respective alloy was investigated, of which result is in Fig. 14. An excellent correlation between them is found,

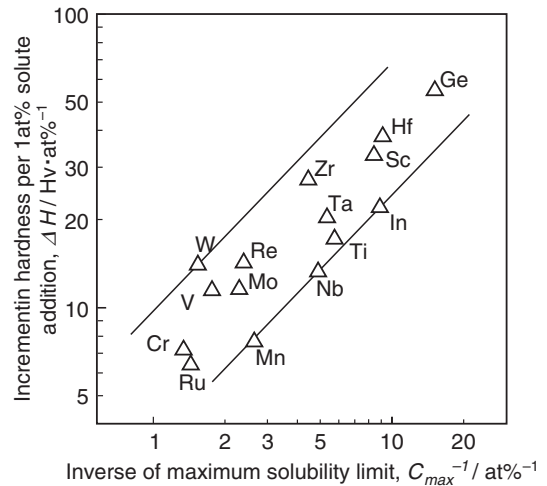


Fig. 14 Relationship between the inverse of the maximum solubility limit and the increment in hardness per 1 at% solute addition in Pt-based binary alloys.

although a scatter band is rather broad. This result indicates that solid solution hardening in the binary alloy with the narrow solubility limit becomes larger compared with that of the alloy with the wider solubility limit. Solubility limits of Ge and Hf in Pt-based binary alloys are relatively narrow as 6.7 at% and 11.0 at%, respectively, and so these solutes give rise to the largest solid solution hardening. Shinoda *et al.* analyzed an extra hardening observed in Ni-based alloys with the solubility limit based on the heat of formation for solid solution, and found that this heat of formation became higher in alloys with the larger size misfit, while it was very low and independent of the size misfit in a completely miscible type of alloys.<sup>18)</sup> They concluded that this was well correlated with an atomic interaction parameter between solute and solvent atoms.

As shown in Fig. 7, the increment of hardness in a respective solute element appears to be related to the periodic group number or the crystal structure of the solute element. Mishima *et al.* reported that an extra hardening of solid solution hardening observed by addition of transition metals elements in nickel was caused by a possible contribution of electronic interaction involving d-electrons.<sup>17)</sup> As already noted, d-electron character is associated with various properties including the cohesive bond strength between atoms, and so the periodic table or d-electron character appears to be related to the size misfit and the solubility limit which control hardening in solid solution alloys.

## 5. Conclusions

The effects of 25 kinds of solute elements on hardness and grain size in Pt-based binary alloys annealed at 1373 K were investigated together with hardness variations with cold rolling reductions. The following results were obtained.

- (1) All binary alloys evolved the single phase microstructure with an equiaxed grain, and grain size varies in a wide range from 610  $\mu\text{m}$  in pure platinum to 33  $\mu\text{m}$  in Pt-2.5%Mo and Pt-10.8% Ru alloys.

- (2) The decrement of grain size per 1 at% solute addition was evaluated based on grain size difference between pure platinum and a respective alloy. A variation of this value with the solute concentration results on marked reduction in the low solute concentration range below 5 at%, followed by a sluggish reduction in the higher solute concentration range.
- (3) Solid solution hardening was evaluated by the increment in hardness per 1 at% solute addition, which was analyzed based on the size misfit calculated by the measured lattice constants of pure platinum and alloys. While solid solution hardening increases with the increase in the size misfit in all binary alloys, this behavior is clearly classified by the type of binary alloys whether they are completely miscible type or have the solubility limit.
- (4) Solid solution hardening in the binary alloy with the solubility limit is much larger than that of the completely miscible type of the alloy, and the increment of hardness in the former type alloy becomes larger with the higher inverse value of the solubility limit.
- (5) Both values of the decrement of grain size and the increment of hardness obtained in a respective alloy appears to be associated with the periodic number and the group number in the periodic table to which the solute element belongs as well as crystal structure of the solute element, but the more detail investigations are needed to reconfirm these findings and to pursuit the cause for these correlations.
- (6) The superior cold workability is obtained under a cold rolling reduction up to around 70% in all alloys. Work hardening behavior evaluated by variations of hardness with cold rolling reductions is very similar among various binary alloys.

### Acknowledgment

The authors are grateful to MURAO CO., LTD. for a financial support for this study as well as a plenty supply of pure platinum used in this work.

### REFERENCES

- 1) N. Hongou and Y. Tada: *Science of noble metals*, a part of application (Tanaka Kikinzoku Kogyo K.K, Tokyo, 2001) pp. 2–3. (in Japanese)
- 2) T. Okabe: *Kinzoku* **76** (2006) 980–984.
- 3) M. Min, J. Cho, K. Cho and H. Kim: *Electrochim. Acta* **45** (2000) 4211–4217.
- 4) T. Biggs, S. S. Taylor and E. van der Linden: *Platinum Metals Rev.* **49** (2005) 2–15.
- 5) P. J. Hill, T. Yamabe-Mitarai and I. M. Wolff: *Scri. Mater.* **44** (2001) 43–48.
- 6) P. J. Hill, T. Biggs, P. Ellis, J. Hohls, S. Taylor and I. M. Wolff: *Mat. Sci. Eng.* **A301** (2001) 167–179.
- 7) P. J. Hill, N. Adams, T. Biggs, P. Ellis, J. Hohls, S. Taylor and I. M. Wolff: *Mat. Sci. Eng.* **A329–331** (2002) 295–304.
- 8) Z. M. Rdzawski and J. P. Stobrawa: *Mater. Processing Tech.* **153–154** (2004) 681–687.
- 9) B. D. Cullity: *Elements of X-ray diffraction*, translated by G. Matsumura, (Agune Co., Tokyo, 1991) pp. 325–346. (in Japanese)
- 10) S. L. Wang and L. E. Murr: *Metallography* **13** (1980) 203–224.
- 11) T. Nishizawa: *Mater. Trans.* **42** (2001) 2027–2032.
- 12) F. Togashi and T. Nishizawa: *J. Jpn Inst. Metals* **40** (1976) 12–21.
- 13) N. Ohkubo, K. Miyakusu, Y. Uematsu and H. Kimure: *ISIJ Int.* **34** (1994) 764–772.
- 14) F. R. N. Nabarro: *Pro. Phys. Soc. London*, **58** (1946) 669–676.
- 15) E. A. Brandes and G. B. Brook: *Smithells Metals Reference Book*, 7th ed, (Butterworth-Heinemann, London, 1992) pp. 6–9.
- 16) H. W. King: *J. Mater. Sci.* **1** (1966) 79–90.
- 17) Y. Mishima, S. Ochiai, N. Hamano, Y. Yodogawa and T. Suzuki: *Trans. JIM* **27** (1986) 656–664.
- 18) T. Shinoda, G. Choi, Y. Mishima and T. Suzuki: *Tetsu-to-Hagane*: **76** (1990) 1720–1726.
- 19) G. Choi, T. Shinoda, Y. Mishima and T. Suzuki: *ISIJ Int.* **30** (1990) 248–254.